Production of ρ^0 mesons with large p_T at next-to-leading order in heavy-ion collisions

Wei Dai,[1] Ben-Wei Zhang,[2,*] and Enke Wang[2]

[1]*School of Mathematics and Physics, China University of Geosciences (Wuhan), Wuhan 430074, China*

[2]*Key Laboratory of Quark and Lepton Physics (MOE) and Institute of Particle Physics, Central China Normal University, Wuhan 430079, China*

Production of large transverse momentum ρ^0 meson in high-energy nuclear collisions is investigated for the first time at next to leading order (NLO) in the QCD improved parton model. The ρ^0 fragmentation functions (FFs) in vacuum at any scale Q are obtained, by evolving a newly developed initial parametrization of ρ^0 FFs at a scale $Q_0^2 = 1.5$ GeV^2 from a broken SU(3) model through NLO Dokshitzer–Gribov–Lipatov–Altarelli–Parisi (DGLAP) equations. The numerical simulations of p_T spectra of ρ^0 meson in the elementary $p + p$ collisions at NLO give a decent description of STAR $p + p$ data. In $A + A$ reactions the jet quenching effect is taken into account with the higher-twist approach by the medium-modified parton FFs due to gluon radiation in the quark-gluon plasma, whose space-time evolution is described by a (3+1D) hydrodynamical model. The nuclear modification factors for ρ^0 meson and its double ratio with $\pi^\pm$ nuclear modification in central Au + Au collisions at the BNL Relativistic Heavy Ion Collider are calculated and found to be in good agreement with the STAR measurement. Predictions of ρ^0 nuclear modification and the yield ratio ρ^0/π^0 in central Pb+Pb at the CERN Large Hadron Collider are also presented. It is shown that the ratio ρ^0/π^0 in central Pb+Pb will approach to that in $p + p$ reactions when $p_T > 12$ GeV.

A new state of matter of deconfined quarks and gluons, the so-called quark-gluon plasma (QGP), is expected to be created in heavy ion collisions (HIC) at very high colliding energies. To study the creation and properties of the QGP, the jet quenching has been proposed, which states that when an energetic parton traveling through the hot/dense QCD medium, a substantial fraction of its energy should be lost and could in turn be used to obtain the temperature and density information of the QGP [1,2]. Even though rapid developments of experiments and theories on new jet quenching observables, such as dihadron [3,4], photon triggered hadron [5,6], and full jet observable [7–12], have emerged in the last decade, the suppression of inclusive hadron production, as the most intensively studied observable on jet quenching, is still indispensable to unravel the properties of the QCD medium. Recently, by comparing the theoretical calculation with the measurements of the production spectra and its suppression of π mesons which are the most commonly observed hadrons, the jet transport coefficient $\hat{q}$ has been extracted to characterize the local properties of the QCD medium probed by the energetic parton jets [13]. The higher twist multiple scattering of the jet quenching incorporated with perturbative quantum chromodynamics (pQCD) improved parton model has been developed and successfully described the π^0 and η productions and their suppressions in $A + A$ collisions [14–17].

The study of the identified hadron spectra at high p_T other than π^0 and η in HIC can further constrain and cast insight into the hadron suppression pattern. Whereas a relatively large

amount of data on the yields of identified hadrons at large p_T has been accumulated at the BNL Relativistic Heavy Ion Collider (RHIC) and the CERN Large Hadron Collider (LHC) [18–20], there are still very few theoretical studies of hadrons with different types. An interesting type of identified hadrons with available data is the ρ^0 meson, which is heavier than π^0 and η, and also consists of the similar constituent quarks. We notice that even the theoretical calculations of the ρ^0 productions in $p + p$ collisions with large p_T at both the RHIC and the LHC are absent due to the lack of knowledge of parton fragmentation functions (FFs) for ρ_0 in vacuum. In a previous study [16] we have paved the way to understand the identified hadron suppression pattern by calculating the productions of the η meson and investigating the hadron yield ratios [16]. In this article, we extend this study to ρ^0 meson productions and the yield ratios of ρ^0 and π in $A + A$ collisions at the RHIC and the LHC. It is of great interest to see how the alteration of the jet chemistry brought by the jet quenching will eventually affect the ρ^0 production spectrum and the ratio of hadron yields [21–23].

In this paper, first we employ a newly developed initial parametrization of ρ^0 FFs in vacuum at a starting scale $Q_0^2 = 1.5$ GeV^2, which is provided by the SU(3) model of FFs of vector mesons [24,25]. By evolving them through Dokshitzer–Gribov–Lipatov–Altarelli–Parisi (DGLAP) evolution equations at next-to-leading order (NLO) [26], we obtain parton FFs of ρ^0 meson at any hard scale Q. The theoretical results of ρ^0 productions in $p + p$ collisions are provided up to the NLO in pQCD improved parton model, and we find that they describe the experimental data rather well. Then we study ρ^0 production in $A + A$ collisions at both RHIC and

___

*bwzhang@mail.ccnu.edu.cn

LHC by including parton energy loss in the hot/dense QCD medium in the framework of the higher twist approach of jet quenching [27–29]. In this approach, the energy loss due to the multiple scattering suffered by an energetic parton traversing the medium are taken into account by twist-4 processes, and the vacuum fragmentation functions are modified effectively in high-energy nuclear collisions. Therefore, we can compute numerically for the first time ρ^0 meson yields in $A + A$ collisions. We give a description of ρ^0 nuclear modification factor $R_{AA}(\rho^0)$ at large p_T in Au + Au collisions at the RHIC to confront against the experimental data by the STAR Collaboration, and $R_{AA}(\rho^0)$ in Pb + Pb collisions at the LHC to give a theoretical prediction. The double ratio of $R_{AA}(\rho^0)/R_{AA}(\pi^\pm)$ is calculated and found to be in good agreement with the experimental data. Lastly we explore the features of the ρ^0/π^0 ratios in both $p + p$ and $A + A$ collisions.

In the NLO pQCD calculation, the single hadron production can be factorized as the convolution of elementary partonic scattering cross sections up to α^3, parton distribution functions (PDFs) inside the incoming particles, and parton FFs to the final state hadrons [30]. We can express the formula symbolically as

$$\frac{1}{p_T}\frac{d\sigma_h}{dp_T} = \int F_q\left(\frac{p_T}{z_h}\right) D_{q\to h}(z_h, p_T)\frac{dz_h}{z_h^2}$$
$$+ \int F_g\left(\frac{p_T}{z_h}\right) D_{g\to h}(z_h, p_T)\frac{dz_h}{z_h^2} \ . \quad (1)$$

The above equation implies that the hadron yield in a $p + p$ collision will be determined by two factors: the initial (parton-)jet spectrum $F_{q,g}(p_T)$ and the parton fragmentation functions $D_{q,g\to h}(z_h, p_T)$. In the following calculations, we utilize the CTEQ6M parametrization for proton PDFs [31], which has been convoluted with the elementary partonic scattering cross sections up to α^3 to obtain $F_{q,g}(\frac{p_T}{z_h})$. Here, $D_{q,g\to h}(z_h, p_T)$ represents the vacuum parton FFs, which denote the possibilities of scattered quark or gluon fragmenting into hadron h with momentum fraction z_h. They can be given by the corresponding parametrization for different final-state hadrons. So potentially, we could predict all the identified hadron productions in $p + p$ collisions as long as the fragmentation functions are available. Note that the factorization scale, renormalization scale, and fragmentation scale are usually

chosen to be the same and proportional to p_T of the leading hadron in the final state.

To accurately determine the $p + p$ reference, parton FFs in vacuum as a nonperturbative input should be available. So far it is still impossible to derive parton FFs from the first principle of QCD and a common practice is to make phenomenological parametrizations by comparing perturbative QCD calculations with the data. Unlike π and charged hadrons, until now there were very few satisfactory parametrizations of parton FFs for the vector mesons due to the paucity of the relevant data. Fortunately, a broken SU(3) model is recently proposed to provide a systematic description of the vector mesons production [24,25]. To reduce the complexity of the meson octet fragmentation functions, the SU(3) flavor symmetry is introduced with a symmetry breaking parameter. In addition, isospin and charge conjugation invariance of the vector mesons $\rho(\rho^+, \rho^-, \rho^0)$ are assumed to further reduce independent unknown quark FFs into functions named valence (V) and sea (γ). The inputs of valence $V(x, Q_0^2)$, sea $\gamma(x, Q_0^2)$, and gluon $D_g(x, Q_0^2)$ FFs are parametrized into a standard polynomial at a starting low energy scale of $Q_0^2 = 1.5\,\text{GeV}^2$ such as

$$F_i(x) = a_i x^{b_i}(1 - x)^{c_i}(1 + d_i x + e_i x^2). \quad (2)$$

These parameters are systematically fixed by fitting the cross section at NLO with the measurements of LEP (ρ, ω) and SLD (ϕ, $K^\star$) at $\sqrt{s} = 91.2$ GeV. In Refs. [24,25] the parameters of ρ^0 FFs in vacuum at $Q^2 = 1.5\,\text{GeV}^2$ are listed and we obtain ρ^0 FFs at any hard scale $D_{q,g}(x, Q^2)$ $Q > 2$ GeV by evolving them through DGLAP evolution equations at NLO with the computer code invented in Ref. [26], then these ρ_0 FFs $D_{q,g}(x, Q^2)$ are used in our numerical simulations.

We have plotted the parton FFs as functions of fragmenting fraction z_h in the left panel of Fig. 1 at fixed scale of $Q^2 = 100\,\text{GeV}^2$, and also the parton FFs as functions of final state p_T at fixed fragmenting fraction $z_h = 0.6$ in the right panel of Fig. 1. It is observed that at fixed scale ρ^0 FFs decrease with z_h, and the FF of the up quark is much larger than that of the strange quark, especially at large z region. At a typical value with $z_h = 0.6$, we notice that ρ^0 FFs show a rather weak p_T dependence.

The existence of the ρ^0 meson FFs at NLO allows us to calculate the inclusive vector meson productions as a function of the final state hadron p_T in pQCD at the accuracy of NLO. Figure 2 shows the confrontation of the theoretical calculation
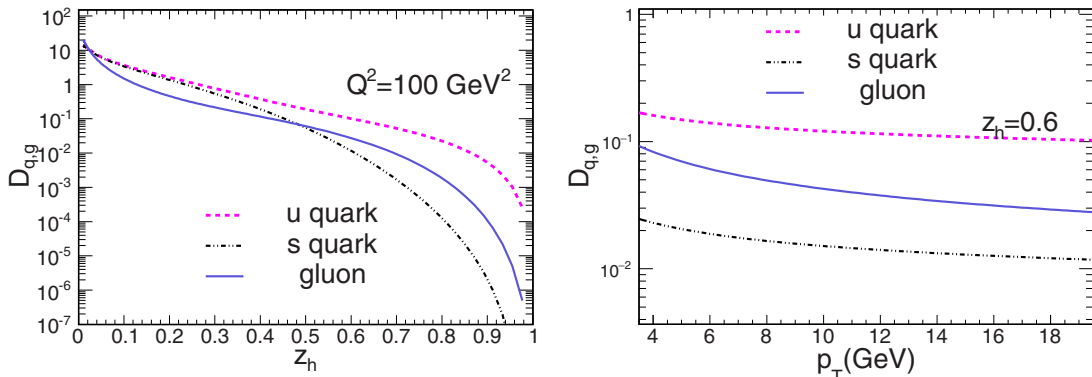

FIG. 1. Left: parton FFs as functions of z_h at fixed scale $Q^2 = 100\,\text{GeV}^2$. Right: parton FFs as functions of p_T at fixed $z_h = 0.6$.
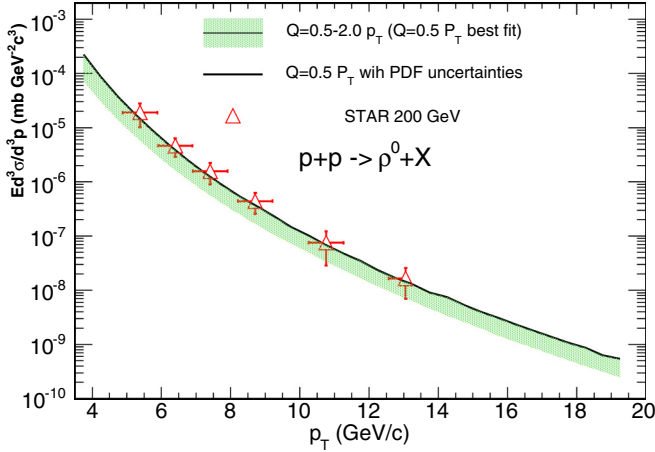
FIG. 2. Numerical calculation of the ρ^0 production in $p + p$ collisions at RHIC 200 GeV compared with STAR [18] data.

with the STAR data [18]. We see the results at the scale $Q = 0.5\,p_T$ agree well with the data of the ρ^0 yield. In the following calculations we will fix $Q = 0.5\,p_T$ to provide a good $p + p$ baseline.

A hot and dense QCD matter is created shortly after the high energy central nucleus-nucleus collisions. Before a fast parton fragmented into identified hadrons in the vacuum, it should suffer energy loss due to multiple scattering with other partons in QCD medium. In the higher twist approach, the multiple scattering is described by twist-4 processes of hard scattering and will lead to effective medium-modification of the vacuum FFs [14–16,27–29,32]:

$$
\tilde{D}_q^h(z_h, Q^2) = D_q^h(z_h, Q^2) + \frac{\alpha_s(Q^2)}{2\pi} \int_0^{Q^2} \frac{d\ell_T^2}{\ell_T^2}
$$
$$
\times \int_{z_h}^1 \frac{dz}{z} \left[\Delta\gamma_{q \to qg}\left(z, x, x_L, \ell_T^2\right) D_q^h\left(\frac{z_h}{z}, Q^2\right) \right.
$$
$$
\left. + \Delta\gamma_{q \to gq}\left(z, x, x_L, \ell_T^2\right) D_g^h\left(\frac{z_h}{z}, Q^2\right) \right], \quad (3)
$$

where $\Delta\gamma_{q \to qg}(z, x, x_L, \ell_T^2)$ and $\Delta\gamma_{q \to gq}(z, x, x_L, \ell_T^2) = \Delta\gamma_{q \to qg}(1 - z, x, x_L, \ell_T^2)$ are the medium modified splitting functions [27–29]. Though the medium-modified FFs include a contribution from gluon radiation in the QCD medium, they obey QCD evolution equations similar to the DGLAP equations for FFs in vacuum. In this formalism, we convolute the medium-induced kernel $\Delta\gamma_{q \to qg}(z, x, x_L, \ell_T^2)$ and $\Delta\gamma_{q \to gq}$ (instead of those vacuum splitting functions) with the (DGLAP) evolved FFs at scale Q^2. We average the above medium modified fragmentation functions over the initial production position and jet propagation direction, scaled by the number of binary nucleon-nucleon collisions at the impact parameter b in $A + A$ collisions to replace the vacuum fragmentation functions in Eq. (1). In the medium modified splitting functions $\Delta\gamma_{q \to qg, gq}$, we can extract the dependency of the properties of the medium into the jet transport parameter $\hat{q}$ which defined as the average squared transverse momentum broadening per unit length. In the higher-twist approach, the jet transport parameter $\hat{q}$ is related to the gluon distribution

density of the medium. Phenomenologically the jet transport parameter can be assumed to be proportional to the local parton density in the QGP phase and also to the hadron density in the hadronic gas phase [14]:

$$
\hat{q}(\tau, r) = \left[\hat{q}_0 \frac{\rho_{\mathrm{QGP}}(\tau, r)}{\rho_{\mathrm{QGP}}(\tau_0, 0)}(1 - f) + \hat{q}_h(\tau, r) f \right] \frac{p^\mu u_\mu}{p_0}, \quad (4)
$$

ρ_{QGP} is the parton (quarks and gluon) density in an ideal gas at a given temperature, $f(\tau, r)$ is the fraction of the hadronic phase as a function of space and time, $\hat{q}_0$ is the jet transport parameter at the center of the bulk medium in the QGP phase at the initial time τ_0 p^μ is the four-momentum of the jet and u^μ is the four flow velocity in the collision frame.

The space-time evolution of the QCD medium is given by a full three-dimensional (3+1D) ideal hydrodynamics description [33,34]. Parton density, temperature, fraction of the hadronic phase, and the four flow velocity at every time-space points are provided by the hydro dynamical model. The only free parameter is $\hat{q}_0\tau_0$, the product of initial value of the jet transport parameter $\hat{q}_0$ and the time τ_0 when the QCD medium is initially formed. This parameter controls the strength of the jet-medium interaction, and the amount of the energy loss of the energetic jets. In the calculations, we use the values of $\hat{q}_0\tau_0$ extracted in the previous studies [14–16], which give very nice descriptions of single π^0 and η productions in HIC. Moreover, we have used the EPS09 parametrization sets of nuclear PDFs $f_{a/A}(x_a, \mu^2)$ to consider the initial-state cold nuclear matter effects [35].

Now we are ready to calculate the single ρ^0 productions in heavy ion collisions up to the NLO. The nuclear modification factor R_{AA} as a function of p_T is calculated to demonstrate the suppression of the production spectrum in $A + A$ collisions relative to that in the $p + p$ collision:

$$
R_{AB}(b) = \frac{d\sigma_{AB}^h/dy d^2 p_T}{N_{bin}^{AB}(b) d\sigma_{pp}^h/dy d^2 p_T}. \quad (5)
$$

In the 0–10 % most central Au + Au collisions at RHIC 200 GeV, we calculate ρ^0 productions at typical values of $\hat{q}_0 = 1.2$ GeV^2/fm and $\tau_0 = 0.6$ fm at the RHIC [16]. The theoretical calculation can explain the data of the ρ^0 meson at a large p_T region (see the top panel of Fig. 3). The theoretical calculation and the experimental data of the π^0 nuclear suppression factor are also presented for comparison. We note that the nuclear suppression factor of ρ^0 is similar to the one of π^0, as demonstrated by the double ratio $R_{AA}^{\rho^0}/R_{AA}^{\pi^\pm}$ in the bottom panel of Fig. 3, which is around 1 calculated at the NLO accuracy. We also find that the theoretical curve undershoots the experimental data of R_{AA}, the same as the case in π^0, and the uncertainty caused by this undershooting will be canceled out to a large extent when we discuss the double ratio of ρ^0 and charged π. Here, $\pi^\pm$ FFs in vacuum are given by AKK08 [38].

To understand better the nature of the suppression pattern of ρ^0, we calculate the gluon (quark) contribution fraction of the total yield both in $p + p$ and Au + Au collisions in Fig. 4. It is similar to η and π^0 productions which demonstrate the domination of the quark fragmentation process contribution at high p_T region either in $p + p$ or in $A + A$ collisions, and
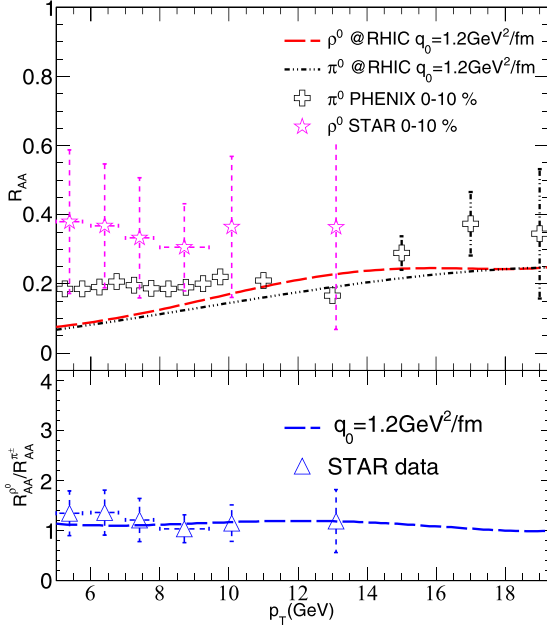
FIG. 3. Top panel: Numerical calculation of the ρ^0 and π^0 production suppression factors in 0–10 % Au + Au collisions at RHIC 200 GeV at NLO as functions of p_T, compared with STAR [18] and PHENIX [36] data. Bottom panel: double ratio calculation of $R_{AA}^{\rho^0}/R_{AA}^{\pi^\pm}$ both at NLO, also compared with STAR data.

the jet quenching effect may suppress the gluon fragmenting contribution but enhance the quark contribution. Therefore the crossing point where the fractional contributions of quark and gluon fragmentation are equal, will move toward lower p_T in the Au + Au collision, as one observes in Fig. 4.

We also predict the ρ^0 production in the 0–10 % most central Pb + Pb collisions at the LHC with $\sqrt{s_{NN}} = 2.76$ TeV in the top panel of Fig. 5. The values of the $\hat{q}_0$ are set to be the same as the typical values which have been used to describe production suppression of both single π^0 and η mesons at the LHC [14–16]. We can see that, with the increase
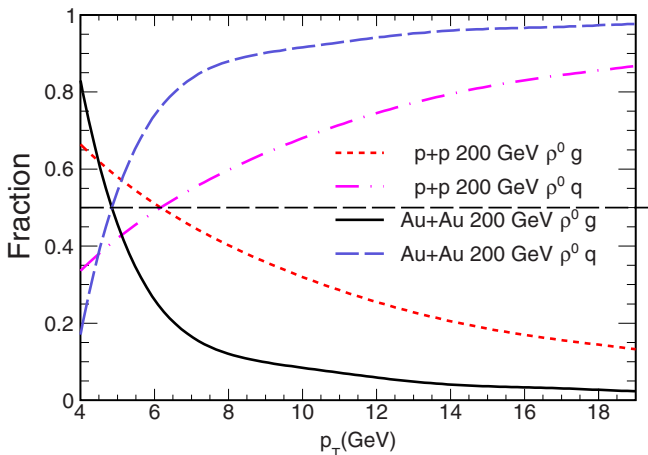

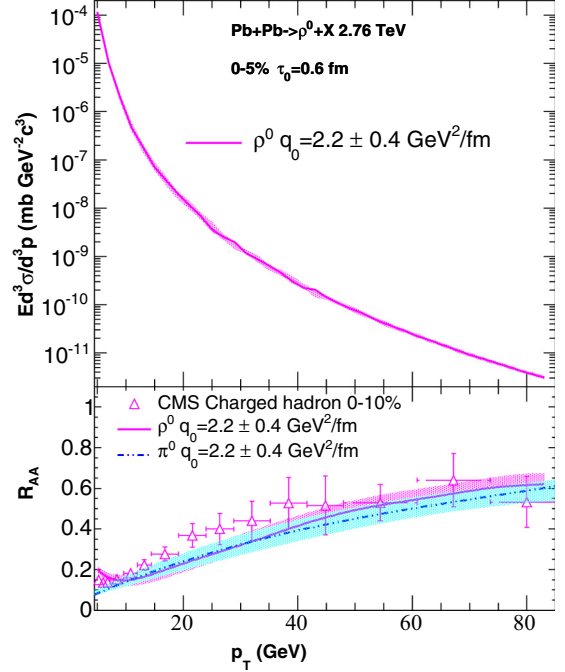FIG. 4. Gluon and quark contribution fraction of the total yield both in $p + p$ and Au+Au at RHIC.

FIG. 5. Numerical calculation of the ρ^0 production in 0–10 % Pb + Pb collisions at LHC 2.76 GeV in the top panel; theoretical calculation results of nuclear suppression factor of ρ^0 and π^0 are compared with the experimental data of charged hadron [37] in 0–10 % Pb + Pb collisions at LHC 2.76 GeV in the bottom panel.

of p_T, the nuclear modification factor of the ρ^0 meson goes up slowly. In the calculation, the best fit to the PHENIX data on π^0 nuclear suppression factor as a function of p_T in 0–5 % Au+Au collisions at $\sqrt{s} = 200$ GeV gives $\hat{q}_0 = 1.20 \pm 0.30$ GeV^2/fm. Similarly, the best fit to the CMS data on charged hadron nuclear suppression factor in 0–5 % Pb+Pb collisions at $\sqrt{s} = 2.76$ TeV as a function of p_T would gives $\hat{q}_0 = 2.2 \pm 0.4$ GeV^2/fm at $\tau_0 = 0.6$ fm/c [13]. The same values of $\hat{q}_0\tau_0$ have been employed to give a very nice description of ρ^0 productions in LHC shown in the bottom panel of Fig. 5.

To compare the different trends of π^0 and ρ^0 spectra, we plot the ratio ρ^0/π^0 as a function of the transverse momentum p_T in Fig. 6. As we have mentioned that in the study the π^0 FFs are given by AKK08 [38]. We note that even the validity of the π^0 (charged hadron) FFs had been challenged by the overpredicting its production in the LHC and Tevatron due to the too hard gluon-to-hadron FFs in the parametrizations [39]. A recent attempt to address the problem and a global refit is performed in Ref. [40]. The uncertainty brought in by the usage of AKK08 fortunately does not affect the results of the nuclear modification factor R_{AA} much due to the cancellation when taking the ratio of $A + A$ production to $p + p$ reference. Therefore one expects that the extraction of jet transport parameter $\hat{q}_0$ from the comparison between the theoretical calculated R_{AA} and the experimental data will not be affected much by such FFs uncertainties. In the studies of particle ratio, π^0 fragmentation function and its jet chemistry are used as reference to understand other mesons such as η, its FFs uncertainties certainly will be expected to affect particle ratios
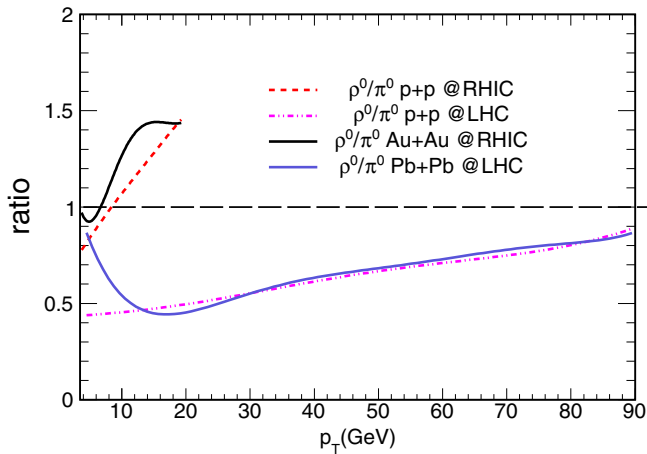
FIG. 6. ρ^0/π^0 production ratio as a function of final state p_T calculated both in $p + p$ and $A + A$ collisions at RHIC and LHC.

like η/π^0. However, since light mesons such as π^0 and η are dominated by quark fragmenting contribution, such effect is therefore minimized.

Figure 6 illustrates that the ratio ρ^0/π^0 increases with the p_T in $p + p$ collisions at the RHIC energy and LHC. Though the jet quenching effect may alter the ratio a little bit in $A + A$ at lower p_T, as p_T becomes larger, the ratio in $A + A$ comes very close to that in $p + p$, especially at the LHC with higher p_T. We note flat curves are observed in η/π^0 ratios as functions of p_T at both the RHIC and the LHC, whereas an increasing ρ^0/π^0 with respect to p_T are shown in Fig. 6. The ρ^0/π^0 ratio in the RHIC demonstrates a more rapidly increasing behavior with respect to p_T. It is realized that the flat particle ratio dependence

of p_T is therefore not a universal trend, and the shape of the particle ratio depends on the relative slope of their spectra in $p + p$, different flavor contributions to FFs as well as flavor dependence of parton energy loss in the QGP.

We note that at high p_T region, the productions of both ρ^0 and π^0 are dominated by quark contribution (for example, see Fig. 4). If at high p_T, quark FFs of ρ^0 and π^0 have a relatively weak dependence on z_h and p_T, then we have

$$
\begin{aligned}
\text{Ratio}(\rho^0/\pi^0) &= \frac{d\sigma_\eta}{dp_T} \bigg/ \frac{d\sigma_{\pi^0}}{dp_T} \\
&\approx \frac{\int F_q\left(\frac{p_T}{z_h}\right) D_{q\to\rho^0}(z_h, p_T)\frac{dz_h}{z_h^2}}{\int F_q\left(\frac{p_T}{z_h}\right) D_{q\to\pi^0}(z_h, p_T)\frac{dz_h}{z_h^2}} \\
&\approx \frac{\Sigma_q D_{q\to\rho^0}(\langle z_h\rangle, p_T)}{\Sigma_q D_{q\to\pi^0}(\langle z_h\rangle, p_T)}.
\end{aligned}
$$

Therefore, while the quark and gluon may lose different fractions of their energies, at very high p_T region, the ratio ρ^0/π^0 in $A + A$ collisions should approximately be determined only by quark FFs in vacuum with the p_T shift because of the parton energy loss. As we can see in Fig. 1, the quark FFs at large scale $Q (=p_T)$ change slowly with the variation of both z_h and p_T, then the ratio of ρ^0/π^0 in both $A + A$ and $p + p$ may approach to each other at larger p_T. It is just as we have observed in the case for the yield ratio of η/π^0 [16].

[1] X. N. Wang and M. Gyulassy, Phys. Rev. Lett. **68**, 1480 (1992).

[2] M. Gyulassy, I. Vitev, X. N. Wang, and B. W. Zhang, in *Quark Gluon Plasma*, edited by R. C. Hwa *et al.* (World Scientific, Singapore, 2003), pp. 123–191.

[3] K. Aamodt *et al.* (ALICE Collaboration), Phys. Rev. Lett. **108**, 092301 (2012).

[4] C. Adler *et al.* (STAR Collaboration), Phys. Rev. Lett. **90**, 082302 (2003).

[5] A. Adare *et al.* (PHENIX Collaboration), Phys. Rev. C **80**, 024908 (2009).

[6] B. I. Abelev *et al.* (STAR Collaboration), Phys. Rev. C **82**, 034909 (2010).

[7] I. Vitev, S. Wicks, and B. W. Zhang, J. High Energy Phys. 11 (2008) 093.

[8] I. Vitev and B. W. Zhang, Phys. Rev. Lett. **104**, 132001 (2010).

[9] W. Dai, I. Vitev, and B. W. Zhang, Phys. Rev. Lett. **110**, 142001 (2013).

[10] G. Aad *et al.* (ATLAS Collaboration), Phys. Rev. Lett. **105**, 252303 (2010).

[11] S. Chatrchyan *et al.* (CMS Collaboration), Phys. Rev. C **84**, 024906 (2011).

[12] Z. B. Kang, R. Lashof-Regas, G. Ovanesyan, P. Saad, and I. Vitev, Phys. Rev. Lett. **114**, 092002 (2015).

[13] K. M. Burke *et al.* (JET Collaboration), Phys. Rev. C **90**, 014909 (2014); Z. Q. Liu, H. Zhang, B. W. Zhang, and E. Wang, Eur. Phys. J. C **76**, 20 (2016).

[14] X. F. Chen, C. Greiner, E. Wang, X. N. Wang, and Z. Xu, Phys. Rev. C **81**, 064908 (2010).

[15] X. F. Chen, T. Hirano, E. Wang, X. N. Wang, and H. Zhang, Phys. Rev. C **84**, 034902 (2011).

[16] W. Dai, X. F. Chen, B. W. Zhang, and E. Wang, Phys. Lett. B **750**, 390 (2015).

[17] W. Dai and B.-W. Zhang, Nucl. Part. Phys. Proc. **289-290**, 433 (2017).

[18] G. Agakishiev *et al.* (STAR Collaboration), Phys. Rev. Lett. **108**, 072302 (2012).

[19] A. Adare *et al.* (PHENIX Collaboration), Phys. Rev. C **83**, 024909 (2011).

[20] R. Bala, I. Bautista, J. Bielcikova, and A. Ortiz, Int. J. Mod. Phys. E **25**, 1642006 (2016).

[21] W. Liu, C. M. Ko, and B. W. Zhang, Phys. Rev. C **75**, 051901(R) (2007).

[22] S. J. Brodsky and A. Sickles, Phys. Lett. B **668**, 111 (2008).

[23] X. Chen, H. Zhang, B. W. Zhang, and E. Wang, J. Phys. **37**, 015004 (2010).

[24] H. Saveetha, D. Indumathi, and S. Mitra, Int. J. Mod. Phys. A **29**, 1450049 (2014).

[25] D. Indumathi and H. Saveetha, Int. J. Mod. Phys. A **27**, 1250103 (2012).

[26] M. Hirai and S. Kumano, Comput. Phys. Commun. **183**, 1002 (2012).

[27] X. Guo and X. N. Wang, Phys. Rev. Lett. **85**, 3591 (2000).

[28] B. W. Zhang and X. N. Wang, Nucl. Phys. A **720**, 429 (2003).

[29] B. W. Zhang, E. Wang, and X. N. Wang, Phys. Rev. Lett. **93**, 072301 (2004); A. Schafer, X. N. Wang, and B. W. Zhang, Nucl. Phys. A **793**, 128 (2007).

[30] N. Kidonakis and J. F. Owens, Phys. Rev. D **63**, 054019 (2001).

[31] H. L. Lai *et al.* (CTEQ Collaboration), Eur. Phys. J. C **12**, 375 (2000).

[32] W. Dai, B. W. Zhang, H. Z. Zhang, E. Wang, and X. F. Chen, Eur. Phys. J. C **77**, 571 (2017).

[33] T. Hirano, Phys. Rev. C **65**, 011901(R) (2001).

[34] T. Hirano and K. Tsuda, Phys. Rev. C **66**, 054905 (2002).

[35] K. J. Eskola, H. Paukkunen, and C. A. Salgado, J. High Energy Phys. 04 (2009) 065.

[36] S. S. Adler *et al.* (PHENIX Collaboration), Phys. Rev. Lett. **91**, 072301 (2003).

[37] K. Aamodt *et al.* (ALICE Collaboration), Phys. Lett. B **696**, 30 (2011).

[38] S. Albino, B. A. Kniehl, and G. Kramer, Nucl. Phys. B **803**, 42 (2008).

[39] D. d'Enterria, K. J. Eskola, I. Helenius, and H. Paukkunen, Nucl. Phys. B **883**, 615 (2014).

[40] D. de Florian, R. Sassot, M. Epele, R. J. Hernández-Pinto, and M. Stratmann, Phys. Rev. D **91**, 014035 (2015).